SIMULATIONS OF TIME RESOLVED EXPERIMENTS IN XUV SPECTRAL RANGE USING TIME GATED ION MICROSCOPY

A Dissertation
Presented to
The Academic Faculty

by

Konstantakis Panagiotis

In Partial Fulfillment
of the Requirements for the Degree of
Bachelor of Science in Physics

University Of Crete
[Octomber 2019]

SIMULATIONS OF TIME RESOLVED EXPERIMENTS IN XUV SPECTRAL RANGE USING TIME GATED ION MICROSCOPY

Approved by:

Dr. Tzallas Paraskevas,
Research Director at
Foundation for Research and Technology -
Hellas Institute of Electronic Structure and Laser

TABLE OF CONTENTS

ABSTRACT

The development of ultra-short laser pulses has led to a plethora of experiments in which light interacts and ionizes atoms and molecules. In those experiments, devices are used to measure the signal due to the ionization in the interaction zone of the light beam with the atoms. However, the spatiotemporal integration, of the measured signal, done by the measurement devices, causes losses in information regarding the ionization dynamics in the interaction volume. Alternatively, this lost information can be gained by using an Ion Microscope and spatially resolving the products of photoionization in the interaction volume of light with gasses. This thesis contains simulations of experiments with XUV-pump-XUV-probe and IR-pump-XUV-probe excitation schemes.

CHAPTER 1. INTRODUCTION

The pump-probe schemes are commonly used approaches for tracing the ultrafast dynamics of matter. The pump pulse excites the system and the probe pulse traces the evolution of the excited system. The latter usually can be achieved by recording the ionization products (ions or electrons) as a function of the delay (τ) between the two pulses. Pump-probe experiments can be performed using co-propagated and counter-propagated beams.

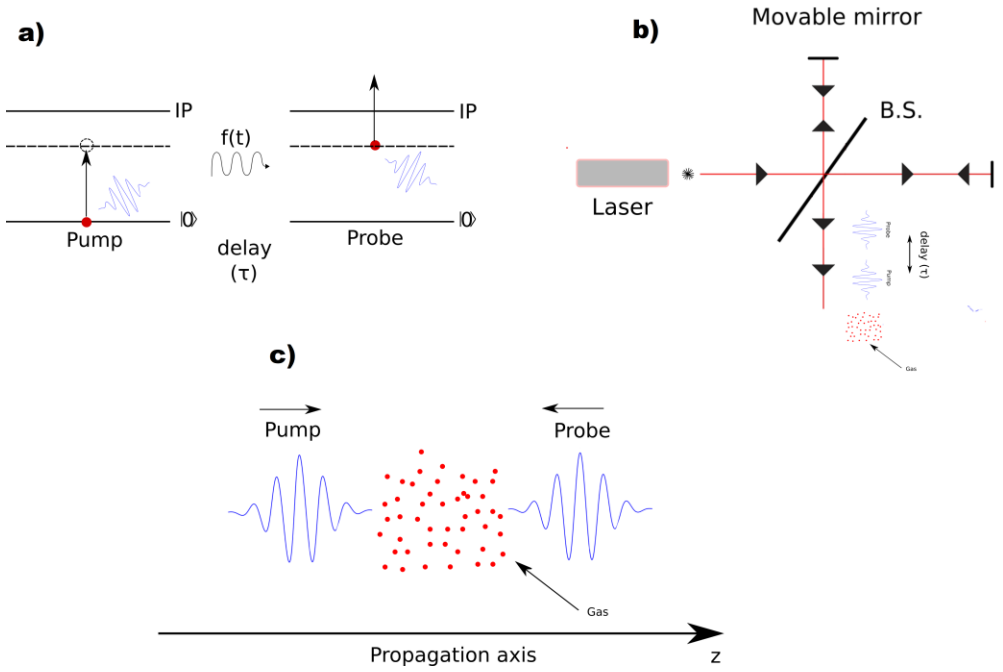

Figure 1. (a) A schematic of the basic principles of pump-probe spectroscopy. An atom is excited by a pulse to a time depended state (pump). The time evolution of the state is recorded by a second pulse that probes the system after a delay time τ and ionizes the atom. **(b)** Pump-probe setup using a Michelson interferometer. In this case, the two pulses co-propagate, and the delay between the two pulses changes as we change the displacement of one of the mirrors This procedure is repeated for many delay times (τ) and we record the ionization products (ions or electrons). **(c)** Two counter-propagated pulses setup where a delay stage does not exist but the delay changes along the propagation axis z as the pulses move through space inside the interaction volume. The delay between the centers of the two pulses is equal to $\tau = z/c$ where z is the distance between them. In the counter propagated beams case we have to spatially resolve photoionization products.

In this thesis, we will present calculations on how we can extract information about the ultrafast dynamics if we spatially resolve ions/electrons distribution inside the interaction volume of counter- propagated XUV-pump-XUV-probe and XUV-pump-IR-probe

beams. In the first section of the thesis are discussed the operation principles of Ion Microscope which is simulated using Simion in section 2. The last section is dedicated to single-shot pump-probe experiments.

.

CHAPTER 2. OPERATIONAL PRINCIPLES OF TIME GATED ION MICROSCOPY

The Ion Microscope is used to record the spatial distribution of the ions or electrons produced on the focus of a tightly focused laser beam. It can produce an image of the spatial distribution of Ions as a function of their mass over charge ratio.

2.1 Setup and operation of Ion Microscope

The basic components of the Ion Microscope are shown in Figure 1. In the beginning, the laser beam is focused on the region between Repeller and Aperture and produces charged particles.

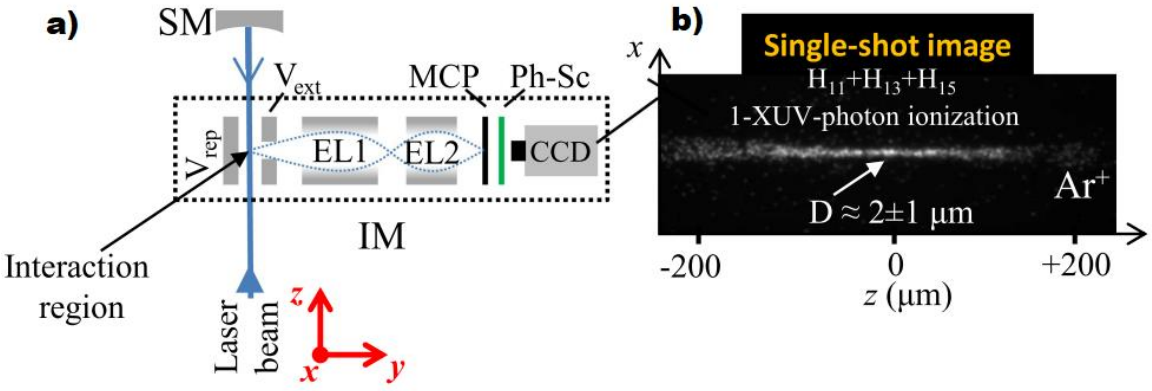

Figure 2.(a) The basic components of the Ion Microscope are shown here. In the beginning, the laser beam is focused on the region between Repeller and Aperture and produces charged particles. **(b)** An image recorded on the MCP when an XUV pulse produced by the interaction of an infrared laser pulse of 30 fs with gas, is focused on Ar gas by a 5cm focal length gold mirror. The XUV pulse that contains harmonics from 11th and 15th ionizes the system, via one-photon ionization, and finally, Ar^+ is produced. Adapted from [3].

Next, the electric field caused by the potential difference between Repeller (V_{rep}) and extract electrodes (V_{ext}), (which are placed in a distance of 0.5 cm from the repeller) accelerates the charged particles towards the electrostatic lens 1. The first electrostatic lens projects a slightly magnified image, of the initial spatial distribution, on Its focal plane with a magnification factor of M_1 (with a magnitude of order between 5 and 7). The second electrostatic lens magnifies further the image with a magnification factor of M_2 (with a magnitude of order between 20 and 30) and the final image is projected on the Micro Channel Plate with a total magnification of $M = M_1 \cdot M_2$. The final image is

recorded with a CCD camera. Each component of the Ion Microscope has a certain voltage value that detects the magnification of the final image. For operation voltages of the Ion Microscope $V_{Rep} \approx 10\ kV$, $V_{Ext} \approx 8.5\ kV$, $V_{EL1} \approx 6.3\ kV$, and $V_{EL2} \approx 8.5\ kV$, the magnification can be up to $M \approx 150$.

CHAPTER 3. SIMION SIMULATIONS OF IONS/ELECTRONS DISTRIBUTIONS

Simion is an Ion and electron optics simulation program that is capable of designing charged particles optics systems like Ion Microscope and running simulations based on those instruments.

3.1 Simion simulations of the Ion Microscope

The manufacturer of the Ion Microscope in order to test and calibrate Ion Microscope made a simple design using Simion 8.1. Based on this manufacturer's design we made a similar model of Ion Microscope on Simion which was used for the simulations of this thesis.

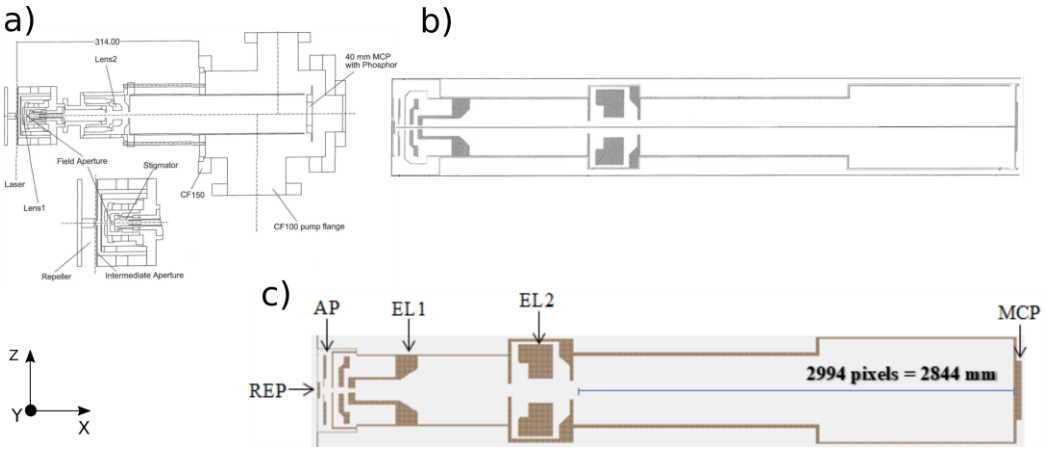

Figure 3. **(a)** This image shows the framework which the manufacturer of the Ion Microscope based the design of his simulation. Ion Microscope has a cylindrical symmetry and here is showed the projection of Ion Microscope on a plane. **(b)** Here is shown the model of Ion Microscope that manufacturer designed using Simion and It is located on the manual of the ion microscope. **(c)** The ion microscope model that we made using Simion based on image (b). The basic components are REP for the Repeller, AP is for the intermediate aperture, EL1 is for electrostatic lens 1, EL2 is for electrostatic lens 2 and MCP is for microchannel plate.

Because the exact dimensions for each component of the Ion Microscope are not known, we had to use an alternative method in order to make a simulation of the Ion Microscope. We started by assuming that the diagram of the ion Microscope inside manufacturer's manual Figure 3 has accurate distance ratios. The next step is to measure the dimensions of each component of the image in pixels and calculate the ratio of mm per pixel. This

ratio is equal to $0.95\ \frac{mm}{pixel}$ and It is calculated by the diameter of the MCP which is known and equal to 40 mm or 38 pixels. After we have measured, the dimensions for each component of the Ion Microscope, we made a similar model using Simion. Each part of the Ion Microscope is made out of electrodes inside Simion's design interface. For different regions of the Ion Microscope (which are made out of electrodes on Simion), we can set unique voltages values. Then Simion proceeds to calculate the electric field inside Ion Microscope by solving La Place equation $\nabla^2 V = 0$ with boundary conditions given by the voltage values for each part of the on Microscope.

3.2 Using Ion Microscope on Simion's Interface

In this section, we will explain how Ion Microscope magnifies and then projects the spatial distribution of charges by demonstrating a simple example on Simion. In Figure 4 we follow the path of two protons as they accelerate from their starting position between the Repeller and the first Apperture towards the MCP after passing both the electrostatic lenses. The voltage values for Ion Microscope are $V_{REP} = 10000\,V$, $V_{AP} = 8475\,V$, $V_{EL1} = 6293\,V$, $V_{EL2} = 8000\,V$.

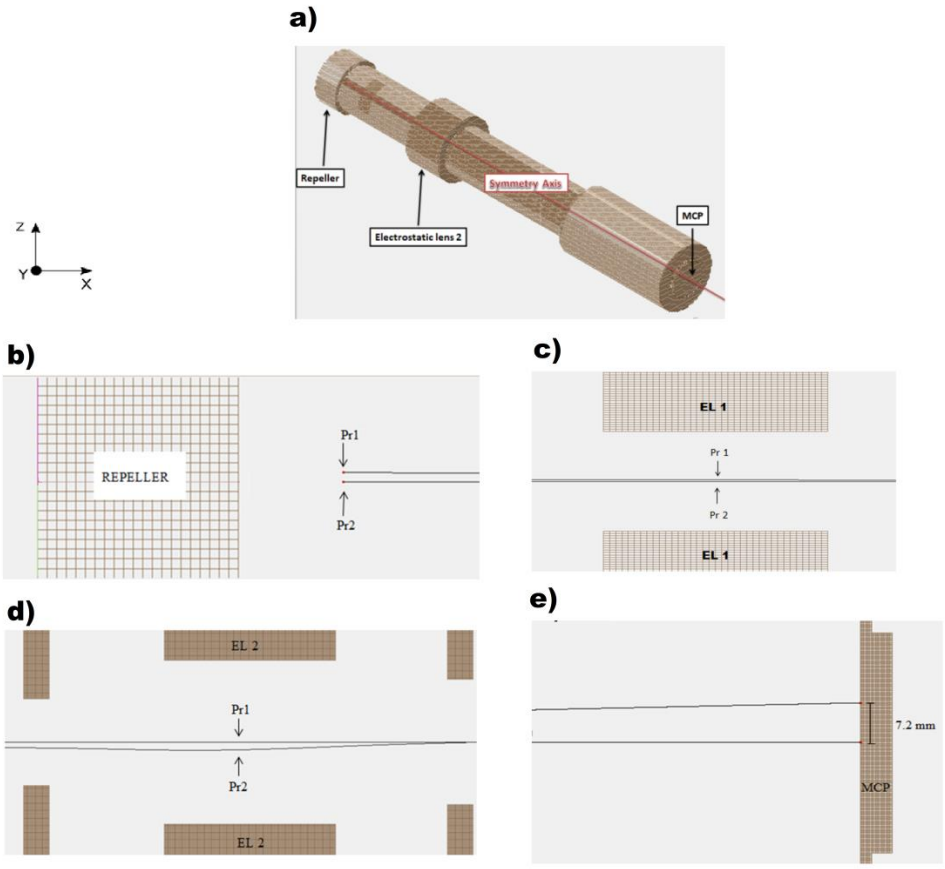

Figure 4. (a) A 3D image of the Ion Microscope with Its symmetry axis (cylindrical symmetry) passing through the center and Its basic components **(b)** Protons (red dots) at the starting position with a distance 0.25 mm from the Repeller. One proton is on the symmetry axis of the Ion Microscope and the other 0.1 mm further away. The two solid lines are their trajectories as they accelerate towards the aperture. **(c**) After protons pass the Aperture, they arrive at electrostatic Lens 1. **(d)** Protons arriving at electrostatic Lens 2. **(e)** Finally, the two protons arrive at the MCP as shown in where the distance between them is 7.2 mm. Knowing the distance of two protons at the beginning and the moment they splat at the MCP we can calculate the magnification factor for these specific voltage values of the Ion Microscope. The magnification factor is equal to the ratio of the final distance to the starting distance of the protons which is equal to $M = \frac{7.2mm}{0.1\,mm} = 72$ **.**

3.3 Simulations using an ion distribution produced at the focus of an XUV focus beam

In order to compare the Ion Microscope model that we made using Simion with the manufacturer's one, we made a simple virtual experiment. The experiment goes like this, an XUV pulse is focused by a mirror between Repeller and the intermediate aperture where we have Argon gas. The XUV pulse profile in space is the same as a Gaussian beam with maximum Intensity of the XUV pulse's maximum intensity. Argon gas is ionized through one-photon ionization and the spatial distribution of Ions is recorded using ion microscope model on Simion. First, the one-photon ionization is simulated by a program written in C++ program language. The program takes as input the volume in space where argon exists, the pressure of the gas, and the temperature. Then proceeds to calculate the number of Argon particles from Ideal Gas Law $PV = Nk_BT \Rightarrow N = \frac{PV}{Nk_B}$ where N is the number of particles, P is the pressure, T is the temperature, V is the total volume, and k_B is the Boltzmann constant. Then the program produces a homogeneous distribution of Argon particles inside this volume. The Ions yield in space depends on XUV beam intensity profile in space and It's given by $\frac{N_{Ions}}{V} \approx 1 - \exp\left(-\frac{I(x,y,z)}{I_{XUV}^{sat}}\right)$ where, $I_{XUV}^{sat} = \hbar\omega_{xuv}/\left(\tau_{xuv}\sigma^{(1)}\right)$ and $\hbar\omega_{xuv}$ is the photon energy at the central frequency o the pulse, $\sigma^{(1)}$is the one-photon ionization cross-section, τ_{XUV} is the pulse duration at FWHM of the XUV pulse. The quantity $1 - \exp\left(-\frac{I(x,y,z)}{I_{XUV}^{sat}}\right)$ is the probability of a particle to become an ion. To obtain the Argon ion distribution in the interaction volume, the software calculates this probability and then compares its value with a uniform distribution set to be in the range between 0 and 1. If the calculated probability is greater than the value chosen from the uniform distribution then the atom becomes an ion. The intensity of the XUV beam around the focus area has a Gaussian Beam profile $I(x,y,z) = I_{XUV}^{max} \cdot \exp\left\{-(x^2+y^2)/\left[w_f^2 \cdot \left(1 + \frac{w_o^2 \cdot z^2}{2 \cdot f^2 \cdot w_f^2}\right)\right]\right\}$, here f is the focal length of the mirror that focuses the beam, $w_0$is the beam diameter, w_f is the beam waist, I_{XUV}^{max} is the maximum intensity of the XUV pulse and z is the propagation axis of the laser. The projection of spatial distribution on the z-y plane of Ions on the focus of the XUV beam can be seen in **Figure 5 (a)**.

3.4 Imaging Ion distribution for different voltage values

Ion Microscope manual contains multiple voltage values combinations that result in different magnifications of the initial distribution of ions in the region of the laser focus. These values were calculated by the manufacturer using Simion and can be seen in Table 1.

Table 1 - Voltage values combinations that result in different magnifications for the Ion Microscope.

Repeller (V)	Aperture (V)	Lens 1 (V)	Lens 2 (V)	Magnification
10000	8475	6270	9000	142
10000	8475	6293	8000	95
10000	8475	6330	7000	50
10000	8475	6409	6000	21

For each combination of voltages of Table 1, we made a simulation using Simion and the Ion Microscope model that we designed. The results are visible in Figure 5 and show what we expect the MCP to record for different magnification factors. In those calculations, the space charge effects due to the repulsion are not accounted for.

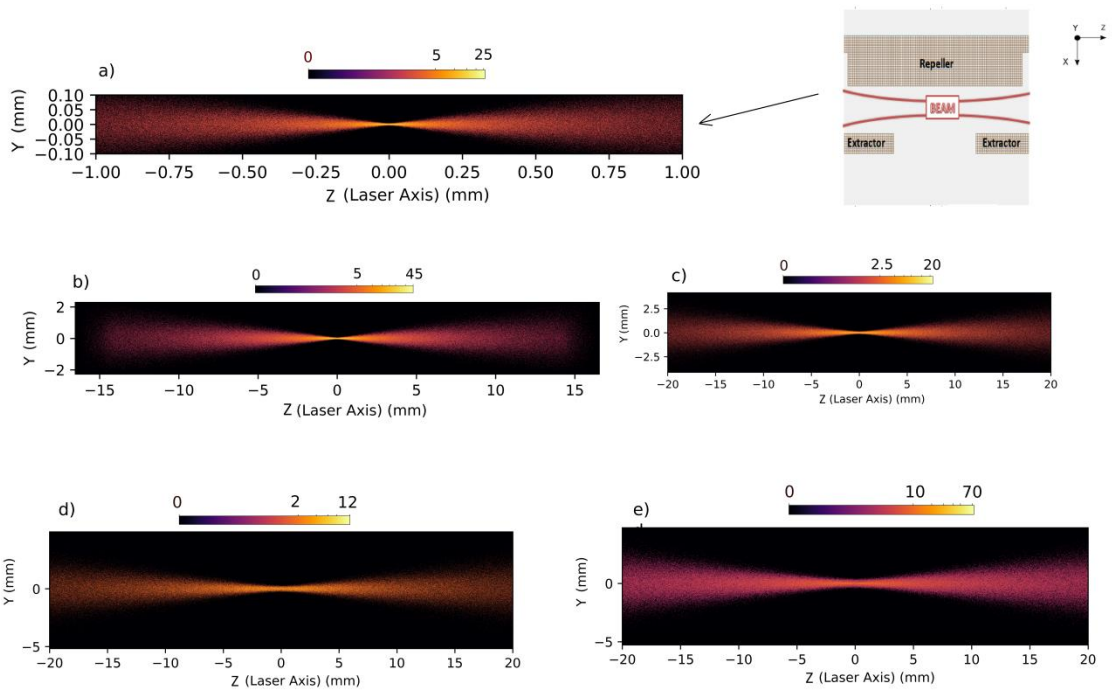

Figure 5. (a) Simulation of an ion distribution produced by a laser beam focused on argon gas between the repeller and the extractor of the Ion Microscope. The values that were used for the simulation are**,** $P = 0.12\,mbar, V = 0.08\,mm^3,$ $N = 2.37191 \cdot 10^9$ particles**,** $T = 20\,°C,$ $\hbar\omega_{xuv} = 23.45\,eV$ (15^{th} harmonic the central frequency of the XUV pulse)**,** $\sigma^{(1)} = 3.3 \cdot 10^{-17}\,cm^2$**,** $\tau_{XUV} = 15\,fs$**,** $f = 50\,mm,$ $w_f = 2\,\mu m$**,** $\mathrm{I}_{\mathrm{XUV}}^{\max} = 2.2 \cdot 10^{13}\,W/cm^2$**.** We can clearly see in this figure the Gaussian profile of the beam. It is noted that because $I_{max} > I_{sat}$ **t**he integrated along the x,y level, Argon ion signal depicts a minimum around $z = 0$ (not shown here) due volume effects in the ionization saturation **area. (b)** Here is shown the magnified image of (a) on the MCP of ion microscope by a magnification factor 21, **(c)** by a factor 50, **(d)** by a factor 95, **(e)** by a factor 142. The voltage values that were used for the previous magnifications are shown in Table 1.

The first part of our simulations is done, the next step is to analyze the images that we gathered from our simulations with Simion. First, we have to compare the theoretical values of magnification of Table 1 with the magnification factor that we calculated from our simulations. So, for Figure 5 we calculate the magnification factor for each ion in relation to the distance from the symmetry axis of the ion microscope. The results for each magnification are shown in **Figure 6**.

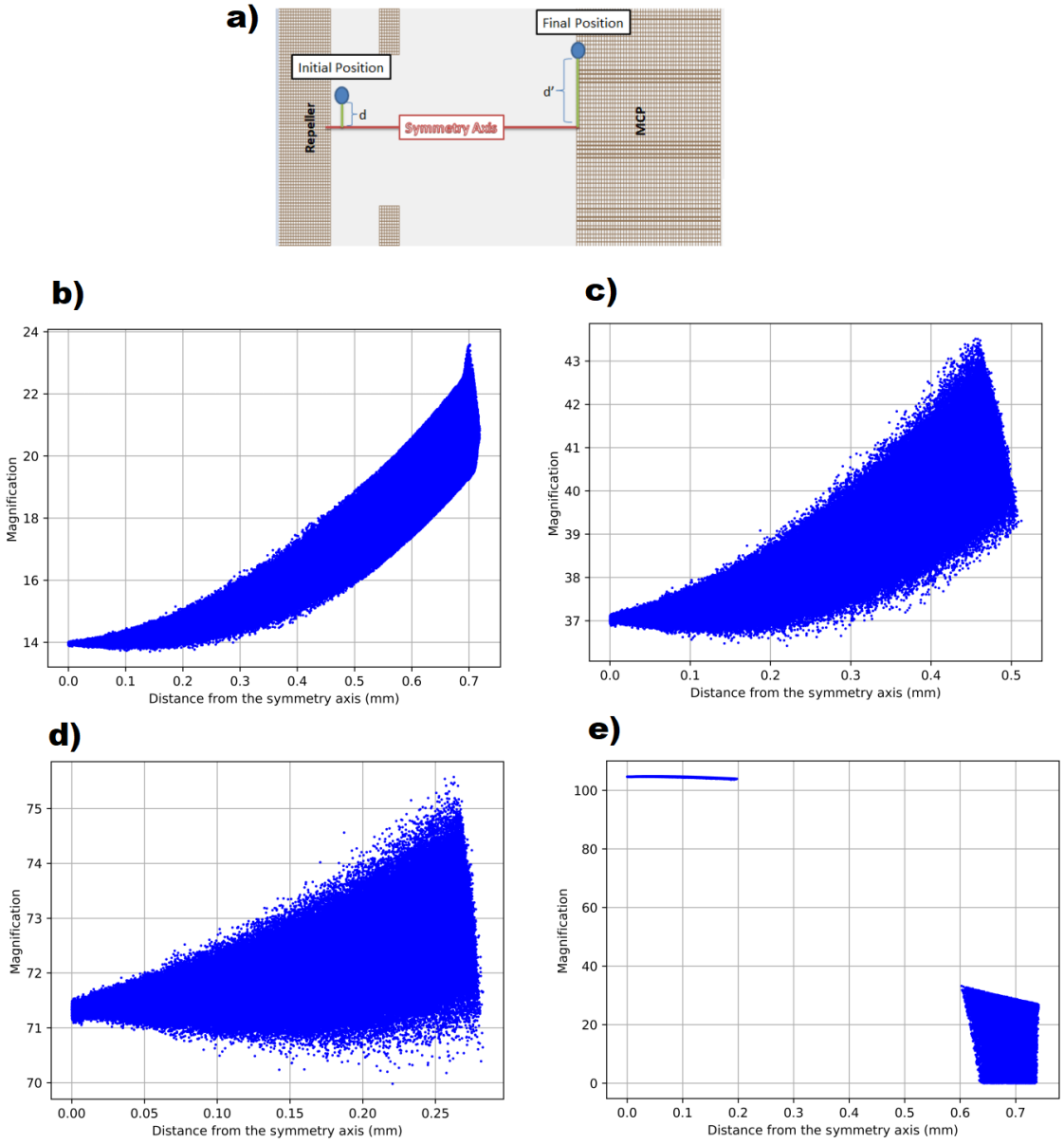

Figure 6. (a) In this image we can see the ion's (blue dot) initial position with distance d from the symmetry axis and Its final position on the MCP with distance d' from the symmetry axis. The Magnification is equal to $M = \frac{d'}{d}$. **(b)** This graph shows the magnification factor dependence calculated by the initial and the final positions of the ions for (b) on Figure 5 projection of ions distribution on the MCP for a magnification factor of 21. **(c)** Magnification factor dependence calculated for (c) on Figure 5 projection of ions distribution on the MCP for a magnification factor of 50. (d) Magnification factor dependence calculated for (d) on Figure 5 projection of ions distribution on the MCP for a magnification factor of 95. **(e)** Magnification factor dependence calculated for (e) on figure 5 projection of ions distribution on the MCP for a magnification factor of 142.

From the previous graphs is very clear that the magnification varies with the initial position of Ions. The magnification is not a single number for a combination of voltage

values but a range of values that depend on the distance of the Ions from the symmetry axis of ion microscope and their distance from the repeller. Further investigation is needed to uncover how magnification changes based on the ions' initial positions.

3.5 The relation between the initial positions of ions and the magnification

In order to test the relationship between the initial position of ions and the magnification of ion microscope, we will place test protons in different positions between repeller and aperture for different voltage values.

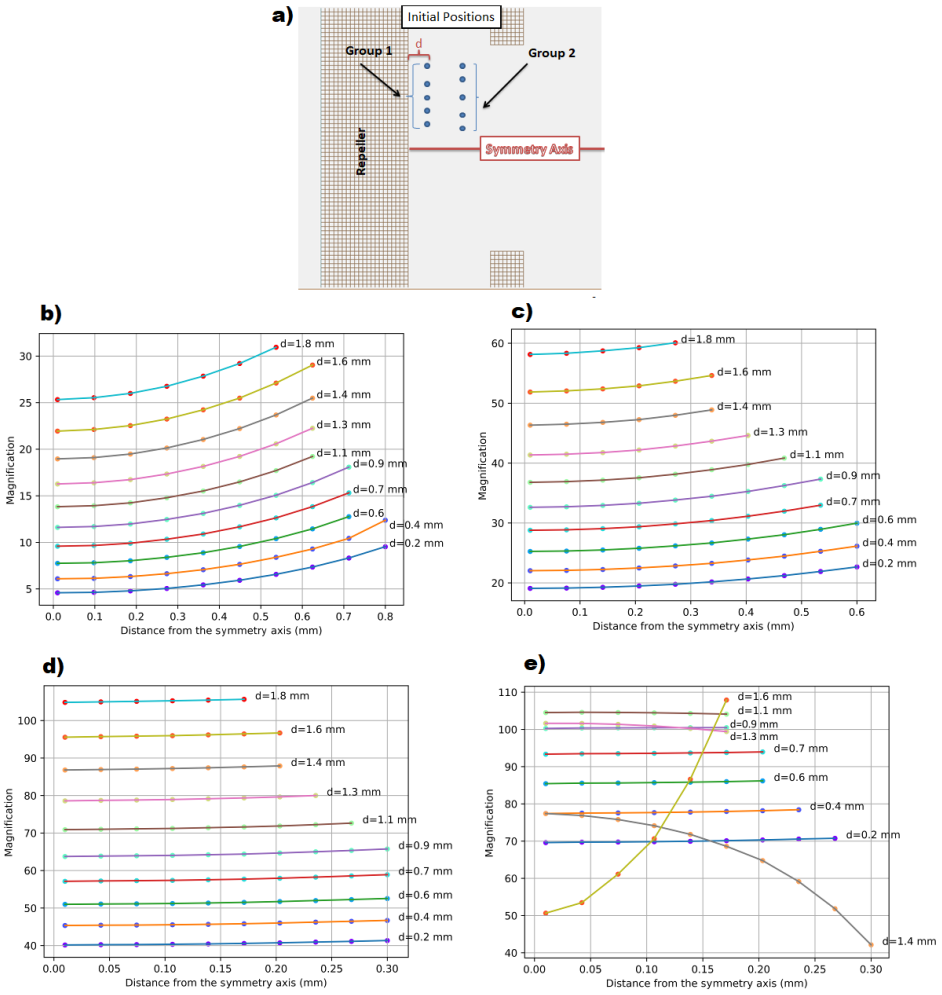

Figure 7. (a) This image shows group 1 of ions in which all the ions have distance *d* from the repeller but ions of the same group have different distances from the symmetry axis. **(b)** This graph shows the magnification of the ion microscope calculated by the initial and the final positions of a few protons. Each line connects dots that correspond to protons that have distance d from the repeller. The first dot on each line corresponds to a proton that has 0.01 mm distance from the symmetry axis of Ion Microscope and this distance increases for the rest of the ions that correspond to the rest dots of the same line. The voltage

values that were used were for a magnification factor of 21, **(c)** for a magnification factor of 50, (d) for a magnification factor of 95, **(e)** for a magnification factor of 142.

From Figure 7, we conclude that as we move the ions further away from the repeller the magnification always increases. The same happens as we move further away from the symmetry axis and the rate of magnification increase is greater as the theoretical magnification decreases. This is easily explained by observing Figure 8.

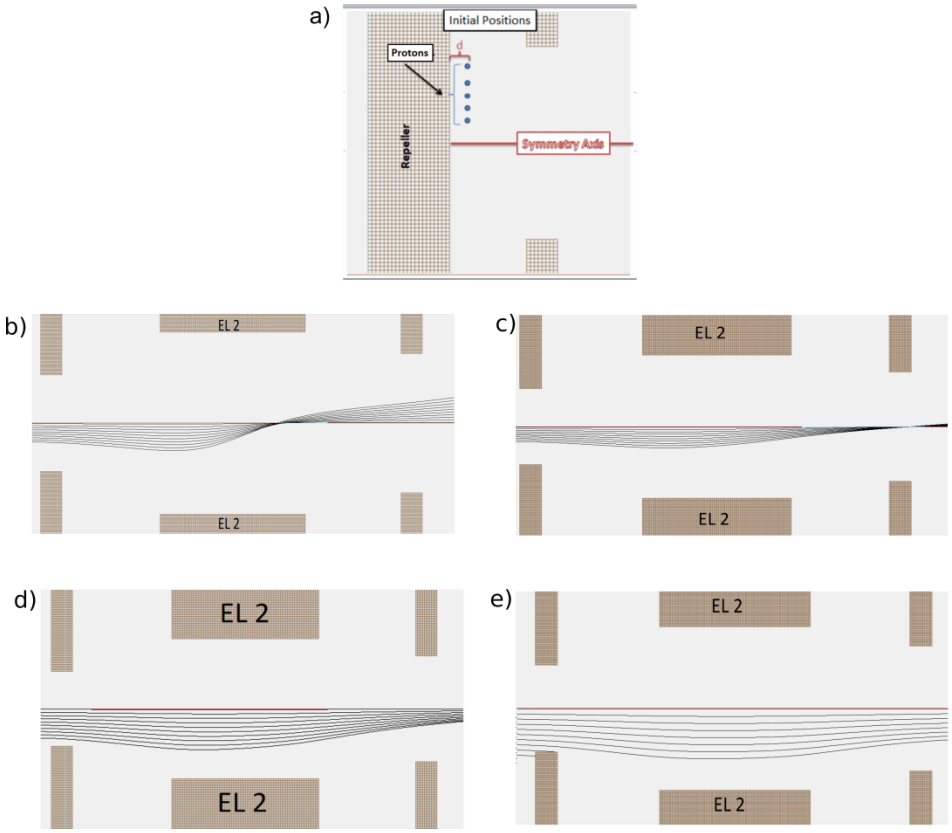

Figure 8. (a) This image shows a group of protons that have distance $d = 1.1\,mm$ from the repeller but different distances from the symmetry axis. The protons are accelerated and then we observe them as they pass from the second electrostatic lens. **(b)** Protons passing through the second electrostatic lens for magnification factor of 21, **(c)** for magnification factor of 50, **(d)** for magnification factor of 95, **(e)** for magnification factor of 142. For lower magnification, the protons fly closer to the surface of the electrostatic lens 2 causing an error similar to the one caused by light when It passes through the edges of an optic lens.

3.6 Testing Simion's space-charge simulation capabilities

Until now all the calculations were done without considering Coulomb repulsion between ions. As the pressure increases the space charge effect in the region of focus of the beam is more intense and becomes apparent by changing the recorded image of the spatial distribution of the ions. With Ion Microscope we can study also the distribution of electrons after photoionization by simply changing the voltage values combinations that we used with ions to negative values. Electrons are more prone to space charge effects because the Coulomb force is the same magnitude of order between them as with the Ions but they have $\approx 1/10^4$ of an Ion's. Simion simulates the repulsion between charges by considering each ion to be an ion cloud with a radius equal to the average distance of all particles. Simion uses a modified version of coulomb law that changes based on the distance of two ion clouds. If the center of an ion cloud is on the center of another ion cloud then the force between them becomes zero. If the distance r between two ions with charge q is the same magnitude of order as the average distance between the particles, the Coulomb force is $F_c \sim q^2/r^2$, if the distance is much larger than the average distance of the particles then $F_c \sim q^2/r$ and if It is much smaller the F_c goes to zero. In order to test Simion's capability to simulate space charge effects, we have a similar setup as the previous section but now we use both Ions and electrons we test Simion capabilities by adjusting parameters like the charge of the particles. The results can be seen in **Figure 9**.

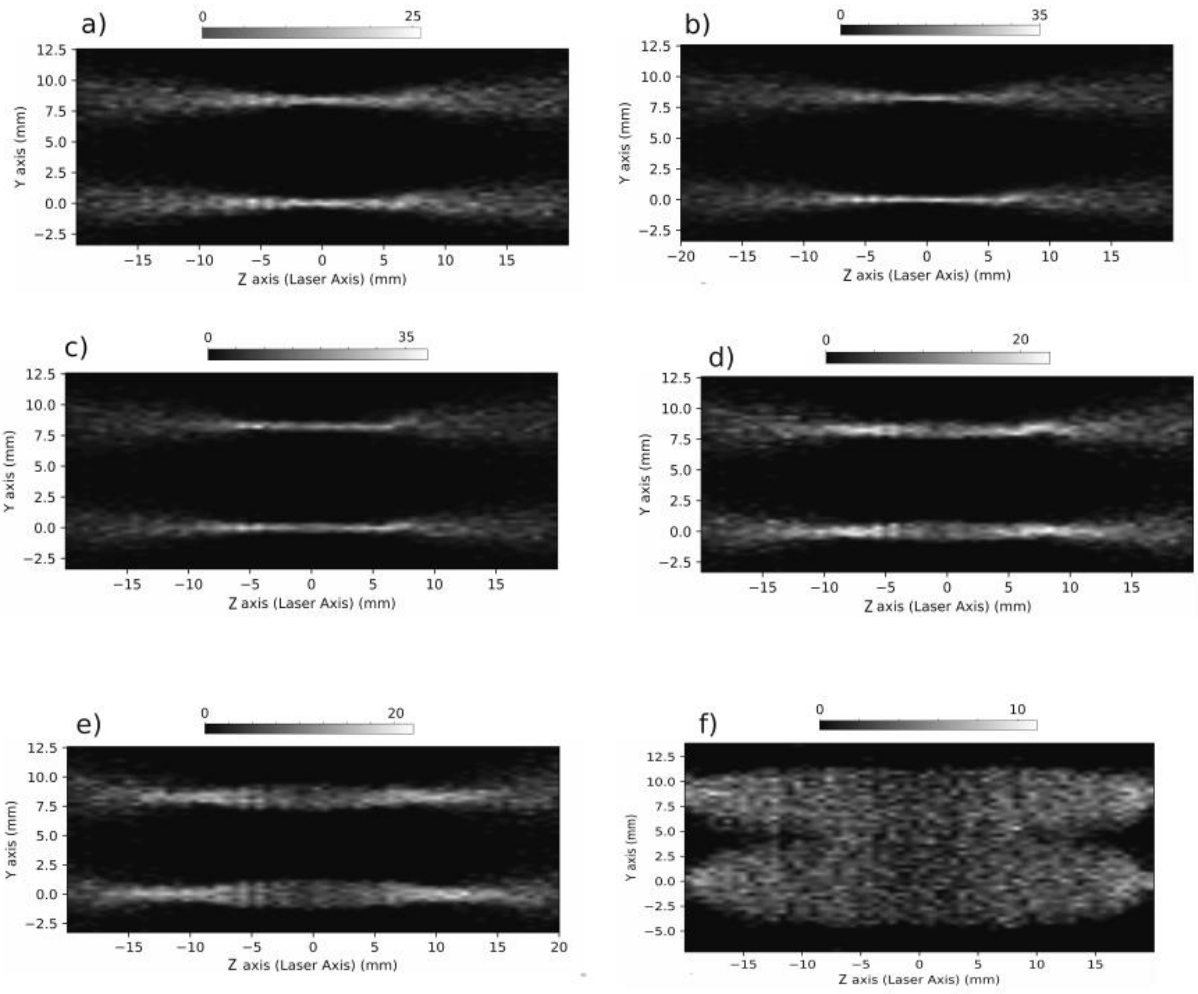

Figure 9. (a) Here is shown the magnified image of an ion distribution on the MCP of ion microscope produced by a laser beam focused on argon gas between the repeller and the extractor. The interaction volume is $V = 0.004\, mm^3$ and pressure is $P = 10^{-6}$ mbar. We present both ions (down) and electrons (up) in the same heatmap but the calculations for ions and electrons were done individually. For each figure, the charge q of Ions and electrons that is used to calculate the repulsion forces is changing from **(a)** zero (no repulsion), **(b)** to 0.01e**, (c)** 0.02e, **(d)** 0.05e**, (e)** 0.1e, **(f**) and 1e. For all the simulations above the XUV beam has σ polarisation and for simplicity, the electrons have initial kinetic energy equal to 10 eV and their momentum is parallel to the positive direction of y axis. The magnification is 142 and the center of the MCP is at $z = 0$**,** $y = 0$.**1**

The results from charge repulsion tests show clearly that Simion 8.0 version is not capable of calculating with precision space charge effects. As we step up the charge of repulsion for each particle there is a huge distortion in the spatial distribution of both Ions and electrons. There are two problems with those observables, the first one is that there are no visible differences between ions and electrons images. Ions are much heavier than electrons and should be less prone to space charge effects. Also, as we have already

mentioned that the pressure is $p = 10^{-6}\, mbar$ which is very low and there is no way to have such a huge distortion on the image as we see in Figure 9 **(f)** where electrons and ions have charge equal to $1e$. The explanation on why Simion fails to calculate space charge effects with accuracy is fairly simple. First, Simion solves La Place equation $\nabla^2 V = 0$ and calculates electric field inside Ion Microscope and the force that is applied by this field to a charge and finally proceeds to add to this force the repulsion from other charges. However, this is accurate only when the charge density is negligible. When charge density increases as for example in the region of the focus of the laser beam, or every time the beam of particles is focused after each electrostatic lens then the more accurate solution is given by Poisson equation $\nabla^2 V = \rho/\varepsilon_o$ where ρ is the charge density and ε_o is the vacuum permittivity. This happens because the flying charges inside Ion microscope change the electric made initially from Ion Microscope.

CHAPTER 4. SIMION SIMULATIONS OF PUMP-PROBE SCHEMES

In this chapter, we will discuss single-shot experiments of XUV-pump-XUV-probe schemes and XUV-pump-IR-probe schemes where the Ion Microscope is used to monitor the interaction between the two pulses and the gas in the interaction region.

4.1 XUV-pump-XUV-probe schemes

The electric field of an ultrashort pulsed Gaussian beam both in time and space can be described mathematically by the following formula

$$E_{GP}(z,t,\omega) = \frac{Ao}{\sqrt{1+\left(\frac{z}{z_o}\right)^2}} \cdot exp\left[-4ln2\,\frac{\left(t-\frac{z}{c}\right)^2}{T^2}\right] \times \cos\left[\omega\cdot\left(t-\frac{z}{c}\right)+\tan^{-1}(z/z_o)\right]$$

Where A_o is the maximum of the electric field of the pulse, z_o is the Rayleigh range at the central frequency of the pulse, T is the duration of the pulse at FWHM, ω is the angular frequency at the central frequency of the pulse and z is the propagation axis of the pulse. The interaction volume that we will study is so small that we can neglect the radial dependence of the electric field. On the other side, an attosecond pulse train can be described simply as the sum of ultrashort pulses with different harmonic frequencies $E_{TP} = \sum_{q=1}^{k} E_{GP}(z,t,\omega_q)$. The first simulation that we will deal with two Attosecond pulses that counter propagate inside Argon gas.

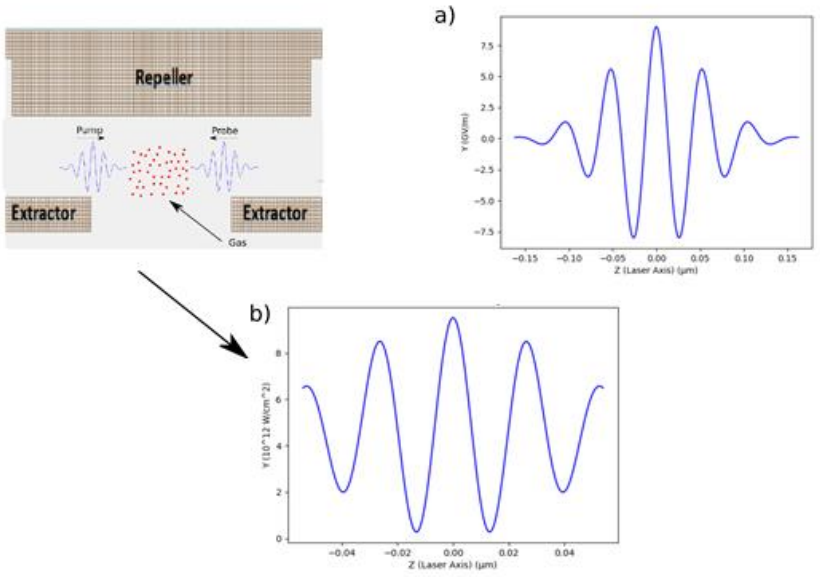

Figure 10. (a) Image of the electric field of each individual attosecond pulse in space with a duration of 300 as, central frequency around the 15^{th} harmonic ($3.5 \cdot 10^{16}\,Hz$), and peak intensity $2.15 \cdot 10^{13}\,W/cm^2$. **(b**) The two pulses pass through each other inside Argon gas that is located between the repeller and aperture of Ion Microscope. The interaction volume $is\ 5 \cdot 10^{-2}\,\mu m^3$ and the pressure is $P = 50\,mbar$**.** Here is shown, the spacial intensity distribution of the electric field in interaction space as the pulses pass through each other. The intensity is calculated by the total electric field using the formula $I = E^2/Z_0$ where $Z_0 = 377\,\Omega$ is the vacuum impedance. It takes about 1.44 fs for both of the pulses to pass through the gas inside the interaction region, that is located between the Repeller and the extractors.

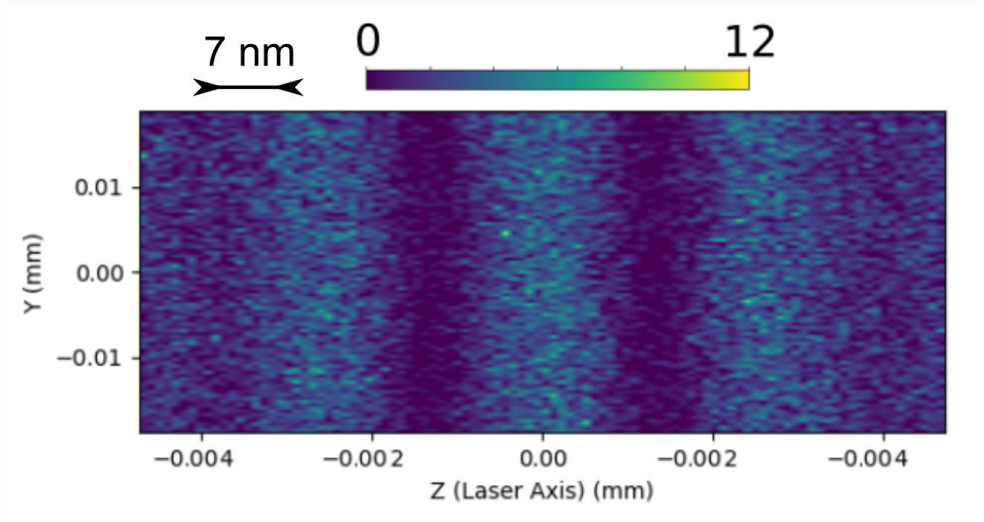

Figure 11. The Argon is ionized through one-photon ionization from the two counter propagated isolated attosecond pulses and the spatial distribution of the ions produced that is projected on the MCP can be seen here. The dark line on the left upper corner shows the distance between two spots in the interaction region if the image wasn't magnified. The theoretical magnification for the combination of voltages values that were used is 142. Space charge effects were not taken into consideration.

As we can clearly see every time the intensity of the electric field increases, the ion production in space increases too. The next part of the experiment is to repeat the same measurement but now we have two trains of attosecond pulses. As we previously mentioned, a train of attosecond pulses is just a sum of ultrashort laser pulses. The XUV is generated by the interaction of IR laser field with gas.

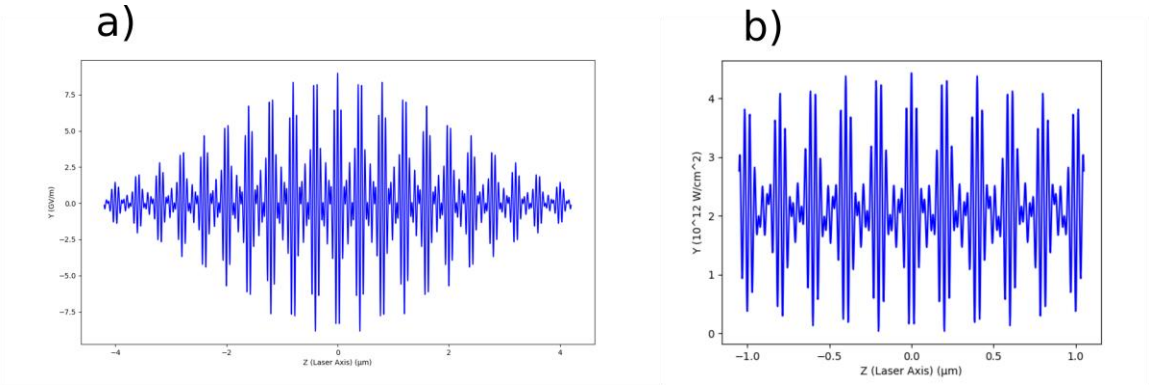

Figure 12 (a) Image of the electric field of the attosecond pulse train which is the sum of three pulses with $T = 11.7\,fs$ at FWHM, $\omega_1 = 2.6 \cdot 10^{16}\,Hz$ (11^{th} Harmonic of the generation IR field), $\omega_2 = 3.5 \cdot 10^{16}\,Hz$ (13^{th} Harmonic)**,** $\omega_3 = 3.1 \cdot 10^{16} Hz$ (15^{th} Harmonic) and the maximum intensity of the attosecond pulse train is $I = 2.15 \cdot 10^{13}\,W/cm^2$**.** The formula for the train of attosecond pulses is $E_{TP}(z,t) = \sum_{q=1}^{3} E_{GP}(z,t,\omega_q)$**. (b)** The two train pulses pass through each other inside Argon gas that is located between the repeller and aperture of Ion Microscope. The interaction volume $is\ 19\,\mu m^3$ and the pressure is $P = 0.12\,mbar$**.** Here is shown, the spacial intensity distribution of the electric field in interaction space as the pulses pass through each other. It takes about 42 fs for the two pulses to pass through each other.

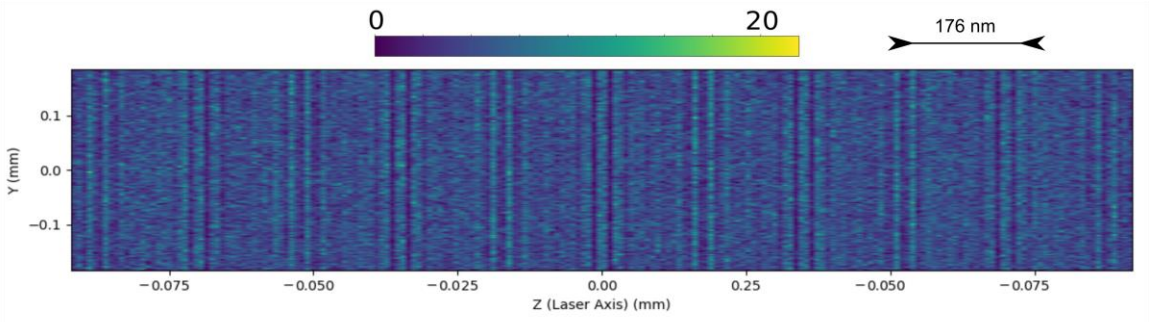

Figure 13 Once again, Argon is ionized through one-photon ionization from the two counter propagated trains of attosecond pulses and the spatial distribution of the electron projected on the MCP can be seen here. The dark line on the right upper corner shows the distance between two spots in the interaction region if the image wasn't magnified. The theoretical magnification for the combination of voltages values that were used is 145. Space charge effects were not taken into consideration.

In Figure 13, we can clearly observe pairs of dark and bright lines due to the rapid oscillations of intensity inside the interaction volume. Those rapid oscillations result in regions (dark lines) on the MCP where the ion yield drops absurdly and spots (bright lines) on the MCP where ion yield increases.

4.2 Time gated photoelectron microscopy in XUV-pump-IR-probe schemes (RABBITT, Streaking)

The first experiment that I will simulate (without considering the space charge effects) has a lot of similarities with the well-known technique of measuring the duration of attosecond pulse trains which is called reconstruction of attosecond beating by interference of two-photon transitions. The technique works by measuring photoelectrons from two-color ionization of a nobble gas from an XUV field complemented by an IR dressing field that was used for the generation of the XUV pulse. In this technique, an XUV train of attosecond pulses that consists of a range of odd harmonics ionizes through one-photon ionization the nobble gas. The energy spectrum of photoelectrons depends on the harmonics that the XUV pulse is constructed with and their intensity. However, due to interaction with the dressing IR field, there is a chance that photoelectrons can also absorb or emit one photon with the frequency of the IR field. The result of this is the interaction is that we observe sidebands on photoelectron energy spectrum between the odd harmonics. The intensity of the sidebands depends on the delay between the XUV pulse and IR field. An example of this can be seen in Figure 14.

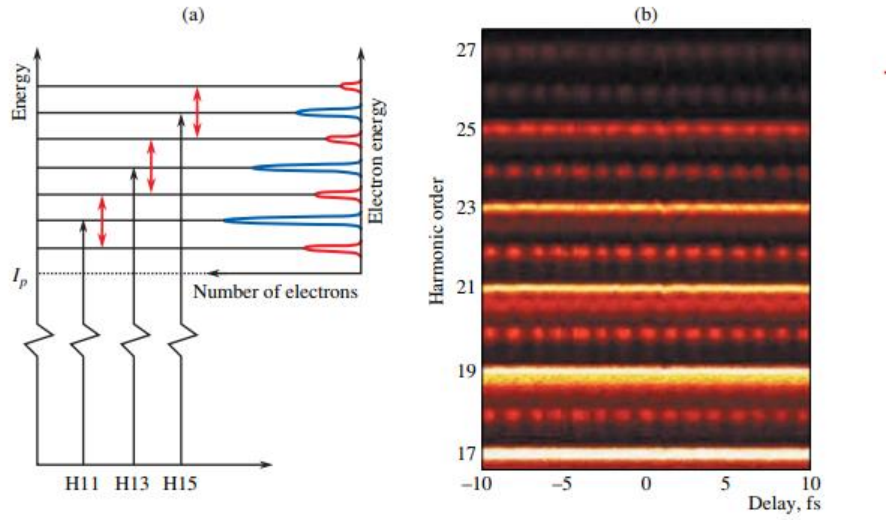

Figure 14. (a) Here is shown the mechanism of the two-photon ionization from the two-color field. First, the electron is ionized by absorbing a photon that corresponds to the harmonics of the XUV field (dark arrows). After the ionization from the XUV field, there is a chance for the photoelectron to absorb or emit a photon of the IR field (red arrow). **(b)** The image shows the photoelectron spectrum measured as the delay changes between the XUV and the IR field. We can clearly observe the oscillations of the intensity of the sidebands between the odd harmonics, while the delay between XUV and IR pulses changes. Adapted from [5].

The intensity of the sidebands is given by the simple formula $I_{2q} = B \cdot \left(I_{2q+1} + I_{2q-1} + \sqrt{I_{2q+1} \cdot I_{2q-1}} \cdot \cos(2 \cdot \omega \cdot \tau + \Delta\varphi)\right)$ where I_{2q} is the intensity of the sideband, $I_{2q+1,}$ and I_{2q-1} are the intensities of the neighbor harmonics and ω is the angular frequency of the IR field, $\Delta\varphi$ is the phase difference between the 2q+1 and 2q-1 harmonics, B is a multiplier factor, τ is the delay between XUV and IR field. For simplicity in our simulation $\Delta\varphi = 0$ and $B = 1$ and $I_{2q+1} = I_{2q-1}$. The intensity of the sideband or a harmonic is proportional to $I \sim E_{el} \cdot N$, where E_{ph} is the photoelectron energy and N, is the number of photoelectrons per unit of time. N can also be interpreted as the probability per unit of time to measure a photoelectron with energy $E_{el.}$ The gas in the interaction region is Argon with $IP_{Ar} = 15.76\ Ev$ and the photoelectrons have energy equal to $E_{el} = \omega_q \cdot \hbar - IP_{Ar}$ where ω_q is the angular frequency of the q^{th} harmonic. The delay between the two pulses after t time interval passes from the zero delay moment is equal to $\tau = 2 \cdot t$, and we expect to see oscillations in space every 200 nm.

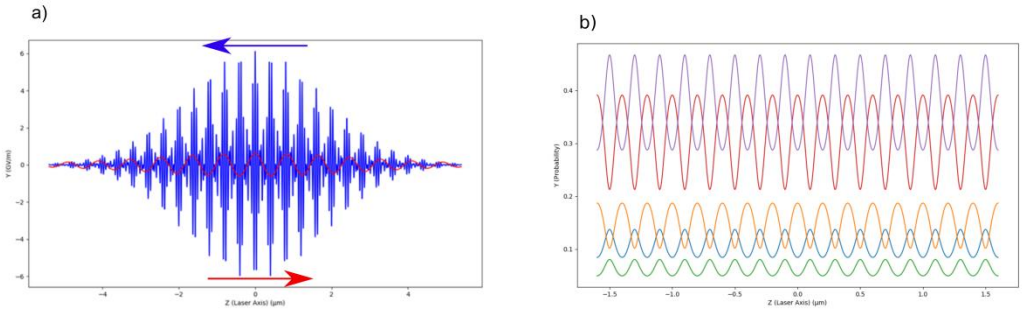

Figure 15 (a) The electric field of the IR (red) and XUV (blue) pulses at the center of the interaction zone (zero delay) as they counter propagate. The angular frequency of the IR field is $\omega = 2.35 \cdot 10^{15}\ Hz$ and the pulse has 20 fs duration at FWHM and maximum intensity equal to 10^{11} W/cm^2. The XUV pulse train consists of a comb of 11th, 13th, 15th harmonics, has a duration equal to 10 fs at FWHM. The maximum intensity is equal to 10^{13} W/cm^2 and the interaction volume is 33 μm^3. **(b)** Probability to observe an electron along z-axis with energy coupled to a certain harmonic. 15th (Green), 14th (Blue), 13th (Orange), 12th (Red), 11th (Purple).

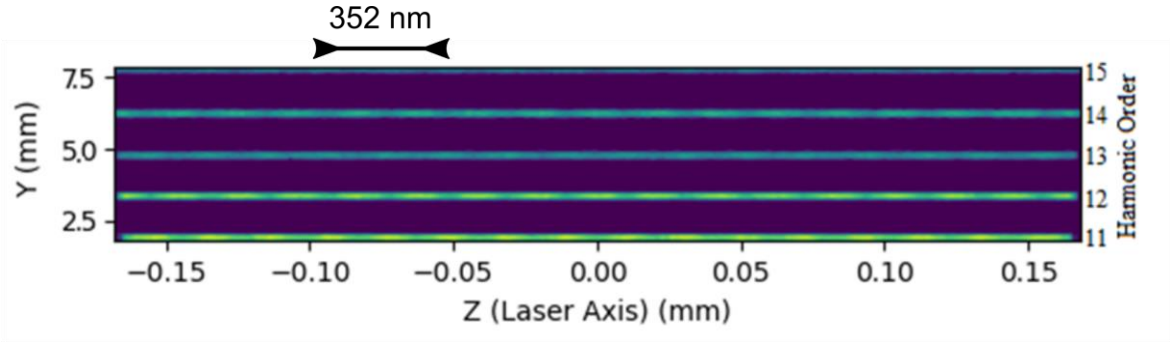

Figure 16. Image on the MCP from two-color ionization of Argon gas by an XUV train of attosecond pulses an/d an IR dressing field. The XUV and IR pulses have σ polarisation and for simplicity, the electrons' momentum is parallel to the positive direction of y-axis. The dark line on the left upper corner shows the distance between two spots in the interaction region if the image wasn't magnified. The Argon gas is located between Repeller and the Apperture of Ion Microscope and the theoretical magnification is 145. The center of the MCP is at $z = 0, y = 0$.

As we can see in the previous figure along y axis we observe that photoelectrons that are coupled to different harmonics result in different lines on the MCP. Along z axis the delay between IR and XUV fields varies and causes the oscillations of the intensity of each line. Last but not least will simulate another experiment that has a lot of similarities with a well-known technique of measuring the duration of isolated attosecond pulses which is called attosecond streaking. In attosecond streaking, an isolated attosecond pulse is focused on a gas target and produces photoelectrons. The XUV pulse is coupled with a strong IR field that modifies the momentum distribution of photoelectrons according to the delay between the IR and XUV field. The change in the momentum of the electrons can be calculated by the formula $p(t_m) = p_0 - eA(t_o)$ where $p(t_m)$ is photoelectron's momentum during the measurement, p_o is the momentum of the electron after ionization, e is the electron's charge and A(t) is the magnetic vector potential. The relation between the magnetic potential and the electric field of the pulse is $A = -\frac{\partial E}{\partial t}$. The effect can be seen in Figure 17.

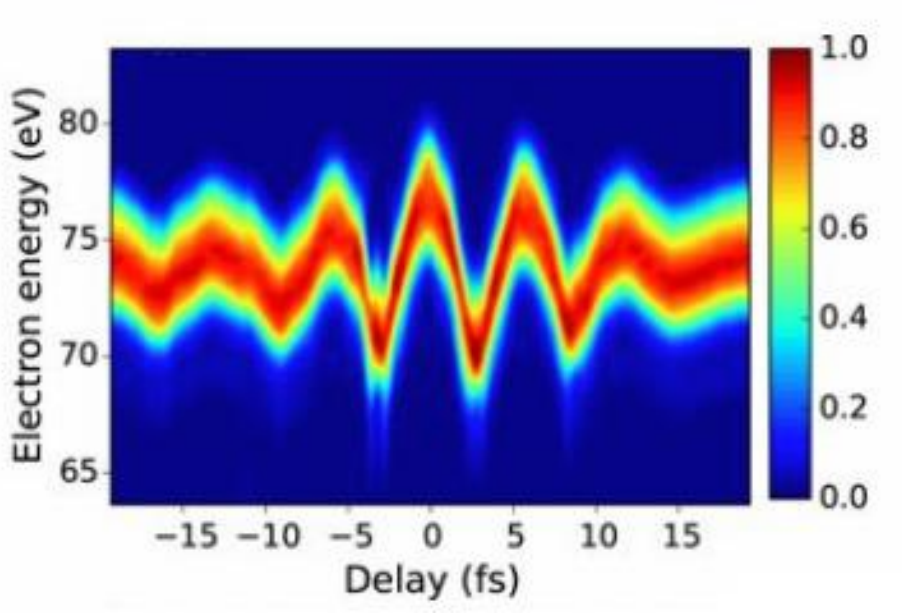

Figure 17. Attosecond streaking measurement with a long-wavelength IR electric field. The photoelectrons' energy distribution changes with the delay between the IR and XUV pulses. The measurement was done and an XUV attosecond pulse. Adapted from [4].

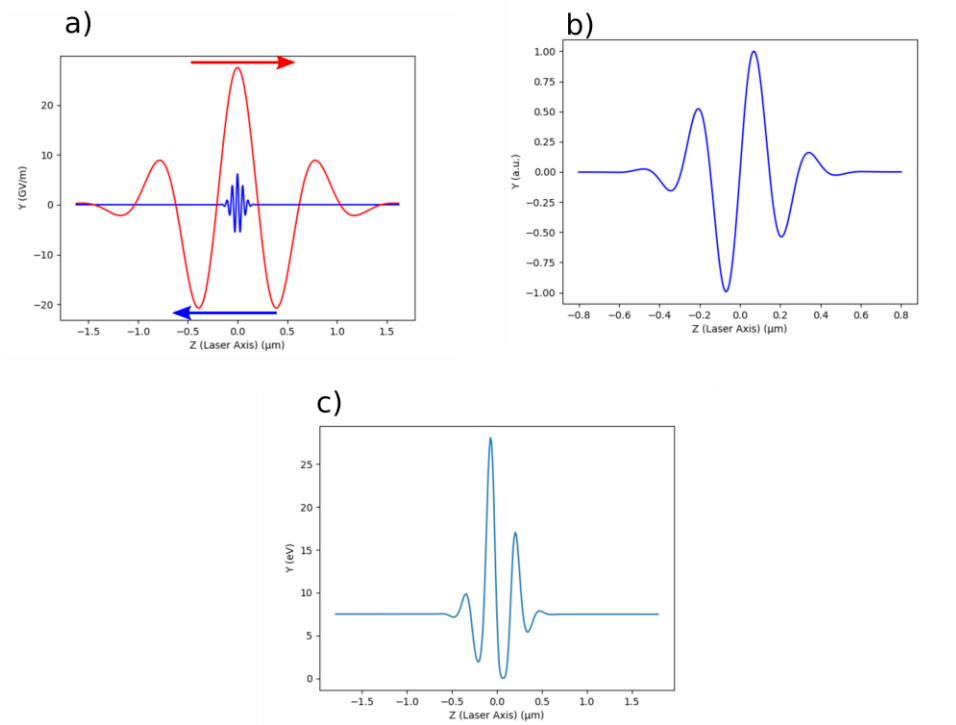

Figure 18. (a) The electric field of the IR (red) and XUV (blue) pulses at the center of the interaction zone (zero delay) as they counter propagate inside Argon gas. The XUV pulse has an angular frequency $\omega = 15 \cdot 1.55/\hbar = 3.5 \cdot 10^{16}\, Hz$ at the central frequency (15^{th} harmonic), T=300 as, and maximum intensity $I = 10^{13}\ W/cm^2$**.** The IR pulse has $T = 3\, fm$ and maximum intensity $I = 2 \cdot 10^{14}\, W/cm^2$. The

interaction volume is $V = 47\,\mu m^3$ and the pressure is equal to $P = 0.1\,mbar$. At the center of the interaction volume for $t = 0$, the delay between the IR and XUV is equal to zero The delay between the two pulses after t time interval passes from the zero delay moment is equal to $\tau = 2 \cdot t$ like in the previous simulation. **(b)** Vector potential of the IR field inside the interaction zone. **(c)** Kinetic energy of photoelectrons in the interaction zone along z axis. The initial kinetic energy of 7.5 eV of photoelectrons changes along z-axis after their interaction with the IR electric field .

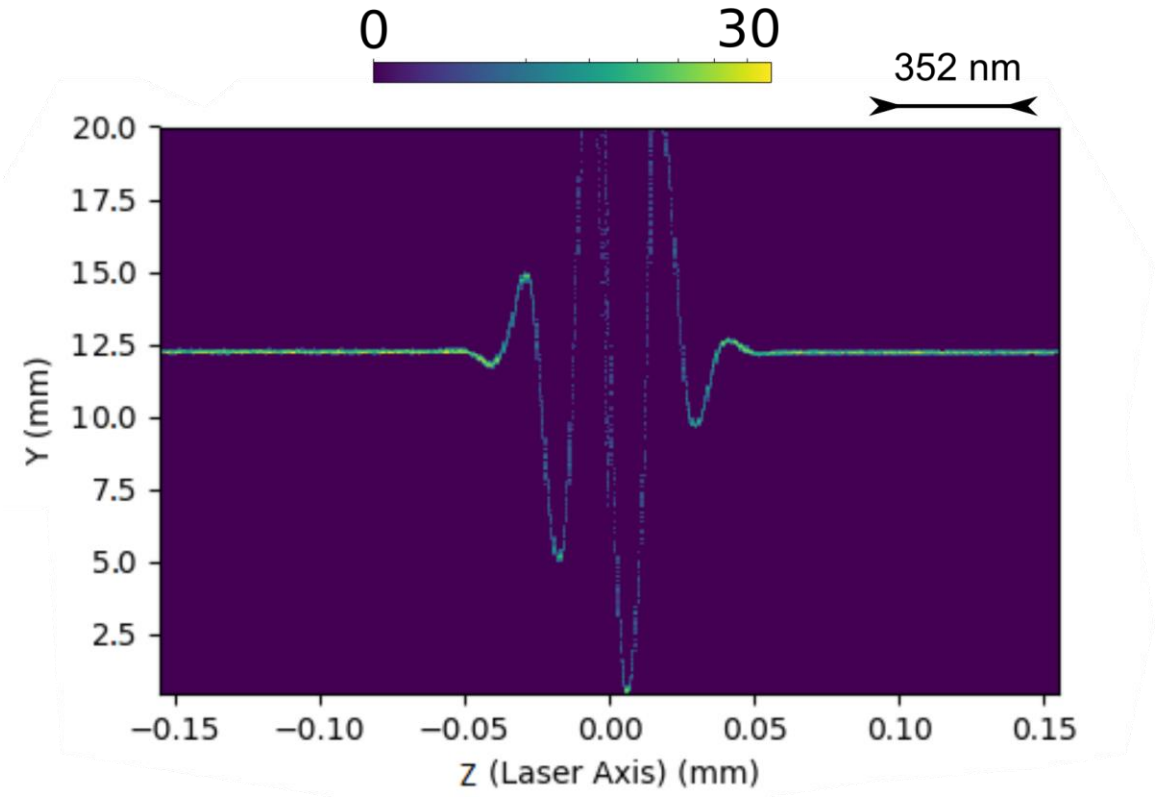

Figure 19. Once again, the XUV and IR pulses have σ polarisation and for simplicity, the electrons' momentum is parallel to the positive direction of y-axis and absorb only the 15th Harmonic. The Argon gas is located between Repeller and the Apperture of Ion Microscope and the theoretical magnification is 145. The center of the MCP is at $z = 0$, $y = 0$. Space charge effects were not taken into consideration. For simplicity, the ionization happens at the center of the XUV pulse as It moves through space. The image of the photoelectrons on the MCP, after their interaction with the IR can be seen here.

In the previous figures we can clearly see that the photoelectrons follow the vector potential of the electric field as the delay between the IR and XUV changes along z axis.

CHAPTER 5. CONCLUSIONS AND OUTLOOK

In this thesis, we managed to design an Ion Microscope model using Simion, study how It performs under various circumstances, simulate XUV-pump-XUV-probe and XUV-pump-IR-probe excitation schemes using time-gated Ion/photoelectron microscopy without taking space charge effects into account. The results show that the attosecond duration and the ultrafast dynamics can be measured in a single shot or multi-shot experiments by recording the spatial distribution of Ions or photoelectrons. Further investigation is required regarding the influence of space charge effects in the measured signal.

REFERENCES

[1] Orfanos, I., Makos, I., Tsatrafyllis, N., Chatziathanasiou, S., Skantzakis, E., Charalambidis, D., & Tzallas, P. (2018). Towards Single-Shot XUV-Pump-XUV-Probe Studies. *Springer Series in Chemical Physics Progress in Ultrafast Intense Laser Science XIV,*209-218.

[2] Tsatrafyllis, N., Bergues, B., Schroeder, H., Veisz, L., Skantzakis, E., Gray, D., . . . Tzallas, P. (2017). The ion microscope as a tool for imaging the ion distribution produced by linear and non-linear processes at the focus of an XUV beam. *2017 Conference on Lasers and Electro-Optics Europe & European Quantum Electronics Conference (CLEO/Europe-EQEC)*.

[3] Tzallas, P., Bergues, B., Rompotis, D., Tsatrafyllis, N., Chatziathanassiou, S., Muschet, A., . . . Charalambidis, D. (2018). Time gated ion microscopy of light-atom interactions. *Journal of Optics,20*(2), 024018.

[4] Saito, N., Ishii, N., Kanai, T., Watanabe, S., & Itatani, J. (2016). Attosecond streaking measurement of extreme ultraviolet pulses using a long-wavelength electric field. *Scientific Reports,6*(1).

[5] Varjú, K., Johnsson, P., López-Martens, R., Remetter, T., Gustafsson, E., Mauritsson, J., ... L'Huillier, A. (2005). Experimental studies of attosecond pulse trains. *Laser Physics, 15(6),* 888-898.

[6] Wang, Z., Zhang, Z., Xu, Z., & Lin, Q. (1997). Space-time profiles of an ultrashort pulsed Gaussian beam. *IEEE Journal of Quantum Electronics, 33*(4), 566–573.

[7] Witzel, B (2018) One XUV Photon Ionization source code (Version 1.0) [Source code]. https://www.researchgate.net/profile/B_Witzel